Effect of variable solubility on reactive dissolution in partially miscible systems

S. Kabbadj,* L. Rongy,† and A. De Wit‡
Nonlinear Physical Chemistry Unit, Université libre de Bruxelles, CP231, Boulevard du Triomphe, 1050 Bruxelles, Belgium

(Received 2 March 2023; accepted 7 June 2023; published 27 June 2023)

When two partially miscible systems are put in contact, one phase, A, can dissolve into the other one with a given solubility. Chemical reactions in the host phase can impact this dissolution by consuming A and by generating products that impact the solubility of A. Here, we study theoretically the optimal conditions for transfer of a reactant A in a host phase containing a species B when a bimolecular $A + B \rightarrow C$ reaction generates a product C that linearly decreases the solubility of A. We have quantified numerically the influence of this variable solubility on the reaction-diffusion (RD) concentration profiles of all species in the host phase, on the temporal evolution of the position of the reaction front, and on the flux of A through the interface. We have also computed the analytical asymptotic concentration profiles, solutions at long times of the RD governing equations. For a fixed negative effect of C on the solubility of A, an increase in the initial concentration of reactant B or an increase in the diffusion rate of species B and C results in a larger flux of A and hence a larger amount of A dissolved in the host solution at a given time. However, when the influence of C on the solubility increases, the mass transfer decreases. Our results help understand to what extent a chemical reaction can optimize the reactive transfer of a solute to a host phase with application to, among other things, the geological sequestration of carbon dioxide in an aquifer.

DOI: 10.1103/PhysRevE.107.065109

I. INTRODUCTION

Transfer between partially miscible (PM) phases in a two-layer stratification has recently attracted renewed interest for understanding convective patterns that develop when a given solute dissolves in a host phase, triggering buoyantly unstable density gradients. This has been observed in the cases of a solid dissolving in a liquid [1,2] and of a gaseous compound dissolving in an aqueous phase [3–10], as well as in two-liquid stratifications [10–15], for instance. In particular, convective dissolution of CO_2 upon its transfer to a host phase in carbon capture and sequestration (CCS) techniques has been the subject of both theoretical [16–24] and experimental [6–8,25–28] works. This convection can be affected by reactions [4–6,14,15,29–35], pressure [27], salinity [8,36], boundary conditions [37], and presence of impurities [38,39].

In the case of reactive systems, it has been shown that, when a species A dissolves in a host phase containing a reactant B, a simple bimolecular $A + B \rightarrow C$ reaction can change the dissolution flux because the reaction modifies the concentration profiles and hence the density stratification at the origin of the buoyancy-driven convection [5,6,29,40–47]. In this context, reaction-diffusion (RD) concentration profiles of A, B, and C have been classified according to the impact of the parameters of the problem on the density profile in the host solution [6,29,40–49].

Most models studying convective dissolution in such PM systems rest on the hypothesis of a constant solubility of A in the host phase [6,14,15,29,31,36,40,41,44–49]. However, solubility depends on pressure [24,27,34,37,50], temperature [36,51], or the concentration of other solutes [36,52], for instance. In particular, in CCS applications, the solubility of carbon dioxide in fluids decreases with decreasing pressure [24,37] and with increasing salinity [36,51,53], which results in less effective convective dissolution of CO_2 in salted solutions [8,54]. Recently, some theoretical studies of reactive convective dissolution made the hypothesis that the reactant A and the product C coexist at the interface, where the sum of the concentrations of A and C is then a constant [42,43]. To the best of our knowledge, the reaction-diffusion base state was not characterized, and the generic influence of a variable solubility on reactive dissolution is still unknown.

In this context, we study theoretically reactive transfer properties between two PM phases when a solute A dissolves in a host phase containing a reactant B and reacts with it according to the reaction $A + B \rightarrow C$, generating a product C that decreases the solubility of A. We study numerically the influence of such a variable solubility of A on the RD concentration profiles, as well as on the temporal evolution of the position of the reaction front and the flux of A through the interface.

This work is structured as follows. The model system and the equations are presented in Sec. II. The numerical results are discussed in Sec. III, along with the analytical solutions corresponding to the asymptotic profiles. An analysis of the temporal evolution of the position of the reaction front and the flux of A entering the host phase is presented in Sec. IV. Finally, conclusions are drawn in Sec. V.

*Sylvain.Kabbadj@ulb.be
†Laurence.Rongy@ulb.be
‡Anne.De.Wit@ulb.be

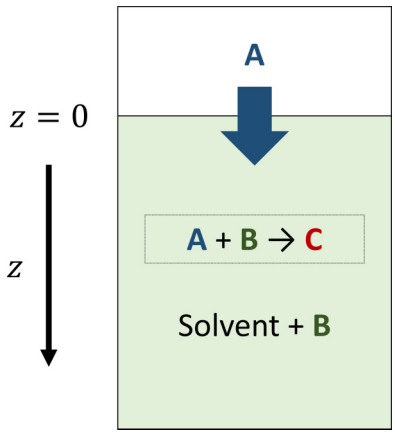

FIG. 1. Schematic of the two-layer partially miscible stratification used to analyze the reactive dissolution of A from the reservoir phase containing pure A into the host phase containing reactant B, where the reaction between A and B produces C.

II. MODEL

We consider an isothermal partially miscible system consisting of a reservoir of A placed above a liquid host phase containing a reactant B. The horizontal planar interface separating the two phases is located at $z = 0$, where z is the vertical axis pointing to the host phase, as represented in Fig. 1. Reactant A dissolves over time with a finite solubility in the host phase, where it reacts with species B with initial concentration B_0, forming product C via the A + B → C reaction. This bimolecular reaction has a reaction rate $v = q\,A\,B$, where q is the kinetic constant and A and B are the concentrations of reactants A and B, respectively.

We consider that the diffusion coefficients are constant, that no mass transfer takes place from the host phase to the reservoir phase, that the density of the fluid is constant, and that the interface is nondeformable. The equations governing the RD evolution of the one-dimensional concentration profiles of species A, B, and C in the host phase are

$$\frac{\partial A}{\partial t} = D_A \frac{\partial^2 A}{\partial z^2} - q\,A\,B, \tag{1a}$$

$$\frac{\partial B}{\partial t} = D_B \frac{\partial^2 B}{\partial z^2} - q\,A\,B, \tag{1b}$$

$$\frac{\partial C}{\partial t} = D_C \frac{\partial^2 C}{\partial z^2} + q\,A\,B, \tag{1c}$$

where D_I is the diffusion coefficient of species I and C is the concentration of product C. The initial conditions are

$$A = A_0 \quad \text{for } z = 0, \quad A = 0 \quad \text{for } z > 0, \tag{2a}$$

$$B = B_0 \quad \forall z, \tag{2b}$$

$$C = 0 \quad \forall z, \tag{2c}$$

where A_0 is the solubility of reactant A in the initial solution of B with concentration B_0 when $C = 0$. Assuming that the solubility of A depends linearly on the concentration of the product C but not on B, the boundary conditions are taken to be

$$A = A_0 - \alpha\,C, \quad \frac{\partial B}{\partial z} = 0, \quad \frac{\partial C}{\partial z} = 0 \quad \text{for } z = 0, \tag{3a}$$

$$A \to 0, \quad B \to B_0, \quad C \to 0 \quad \text{for } z \to \infty, \tag{3b}$$

where α quantifies the influence of C on the solubility of A. The conditions (3b) are used for the analytical analysis of the long time RD solutions. For the numerical simulations at shorter times, we use no flux conditions at $z = L_z$, with L_z being the finite size of the numerical domain along the z axis, taken here to be $L_z = 300$. Note that the choice of L_z does not influence the results provided the system is long enough for the reaction front to be far away from the boundary at $z = L_z$ over the times studied.

The first boundary condition (3a) differs from the constant solubility $A = A_0$ at $z = 0$, i.e., $\alpha = 0$, classically used in the literature for diluted systems [6,14,15,29,31,36,40,41,44–49]. Kim and Cardoso [42,43] used the boundary condition $A = A_0 - C$, i.e., $\alpha = 1$ in Eq. (3a), stating that the diluted reactant A is directly converted into product C by consuming reactant B. In this work, we fix $A = A_0 - \alpha\,C$ and vary α between 0 and 1 to account for the assumption that C linearly decreases the solubility of A, which is the simplest, most general relation.

By using the characteristic RD time and length scales [6,40,44,55,56], $t_c = 1/(q\,A_0)$ and $l_c = \sqrt{D_A\,t_c}$, we introduce the dimensionless time $\tilde{t} = t/t_c$, space coordinate $\tilde{z} = z/l_c$, and concentrations $[\tilde{A}, \tilde{B}, \tilde{C}] = [A, B, C]/A_0$ to nondimensionalize Eq. (1). Dropping tildes for convenience, Eq. (1) become the dimensionless RD system [40]

$$\frac{\partial A}{\partial t} = \frac{\partial^2 A}{\partial z^2} - A\,B, \tag{4a}$$

$$\frac{\partial B}{\partial t} = \delta_B \frac{\partial^2 B}{\partial z^2} - A\,B, \tag{4b}$$

$$\frac{\partial C}{\partial t} = \delta_C \frac{\partial^2 C}{\partial z^2} + A\,B, \tag{4c}$$

where $\delta_I = D_I/D_A$ is the ratio of the diffusion coefficient of species I to that of species A. The dimensionless initial conditions read

$$A = 1 \quad \text{for } z = 0, \quad A = 0 \quad \text{for } z > 0, \tag{5a}$$

$$B = \beta \quad \forall z, \tag{5b}$$

$$C = 0 \quad \forall z, \tag{5c}$$

where $\beta = B_0/A_0$ is the ratio of the initial concentration of B and the solubility of A in the initial solution of B. The dimensionless boundary conditions become

$$A = 1 - \alpha\,C, \quad \frac{\partial B}{\partial z} = 0, \quad \frac{\partial C}{\partial z} = 0 \quad \text{for } z = 0, \tag{6a}$$

$$A \to 0, \quad B \to \beta, \quad C \to 0 \quad \text{for } z \to \infty, \tag{6b}$$

where $A = 1 - \alpha\,C$ is the generic boundary condition used here to describe the influence of the concentration of the product C on the variable solubility of A. The dynamics in the reactive partially miscible two-phase system depends thus on four dimensionless parameters: $0 \leqslant \alpha \leqslant 1$, β, δ_B, and δ_C.

Equations (4)–(6) are integrated numerically by a fourth-order Runge-Kutta method and second-order finite differences with time step $dt = 0.0005$ and space step $dz = 0.05$.

III. RESULTS

To understand the RD dynamics in the host phase, we compute the concentration profiles specific to this partially miscible system and compare them to the nonreactive case, the properties of which are summarized below.

A. Nonreactive case

Upon dissolution of A in a host phase containing no reagent B ($\beta = 0$), i.e., in the pure solvent, the diffusive concentration profile of A is the classical solution of Fick's law $\frac{\partial A}{\partial t} = \frac{\partial^2 A}{\partial z^2}$, with $B = 0 = C$ and the initial [Eq. (5)] and boundary [Eq. (6)] conditions [40]:

$$A_{\mathrm{NR}} = 1 - \mathrm{erf}(\eta), \tag{7}$$

where A_{NR} is the concentration of A in the nonreactive (NR) case and $\mathrm{erf}(\eta)$ is the error function of the self-similar variable $\eta = z/(2\sqrt{t})$. The flux J_{NR} of A dissolving in the host phase through the interface ($z = 0$) in the nonreactive case is given by

$$J_{\mathrm{NR}} = -\left.\frac{\partial A}{\partial z}\right|_{z=0} = \frac{1}{\sqrt{\pi\, t}}. \tag{8}$$

The flux of dissolving A thus decreases in time, as diffusion smooths the concentration gradient [40]. We now investigate how a reaction consuming A affects the dynamics when the reaction product decreases the solubility of A in the host phase.

B. Reactive case

We first study the influence of α on the concentration profiles for $\beta = \delta_B = \delta_C = 1$. Note that summing Eqs. (4b) and (4c) with the given boundary conditions evidences that, if $\delta_B = \delta_C$, we have the conservation relation [6,48]: $B + C = \beta$. If $\beta = 1$, we then have $B = 1 - C$, and since $A(z = 0) = 1 - \alpha\, C(z = 0)$, the interfacial concentrations of A and B are then equal when $\alpha = 1$.

1. Concentration profiles

a. Short times. Figure 2 shows the evolution of the concentration profiles along the z axis at four different times and three values of α. Note that the extent of the z axis differs in the different panels of Fig. 2 for the sake of visual clarity.

A dissolving at the interface diffuses in the host solution and reacts with B to produce C in the reaction zone defined as the region with a nonzero production rate. If the solubility of A is constant ($\alpha = 0$), we recover the profiles that have long been characterized [6,40,44,46,48]; that is, the concentration of A is fixed at the interface ($A = 1$) and decreases monotonically in the host phase. The concentration of B decreases with time at the interface up to $B(z = 0) = 0$, while that of C increases to $C(z = 0) = \gamma$, where γ is the constant concentration of the product C above the reaction front [40]. Note that for $\delta_B = \delta_C = 1$, $\gamma = \beta$. Below the reaction front, B increases from zero to its initial value β, and C decreases from γ to zero.

When $\alpha \neq 0$, the product of the reaction C decreases the solubility of A, and logically, we see in Fig. 2 that, at each time, the concentration of A at the interface is then smaller than $A = 1$. As a consequence, less A diffuses in the bulk, which results in a slower consumption of B and production of C. At the interface, B increases with increasing α, while C decreases. This explains the slower progression of the reaction front (whose position is defined as the point where $A = B$) across the host phase, as seen in Fig. 2. The more C decreases the solubility of A (i.e., the larger α is), the smaller their respective concentrations are at a certain depth z. Conversely, the concentration of B is then larger. Note that, in the specific case with $\alpha = 1$, the concentrations of A and B are equal at the interface when $\beta = \delta_B = \delta_C = 1$, as noted before. Since $A = B$ at $z = 0$, the reaction front is located at the interface in this limit case.

b. Long times. The asymptotic profiles presented in this section are valid for a semi-infinite system or for a system large enough that its length does not influence the results. To obtain the analytical asymptotic solutions of Eqs. (4)–(6) at long times for any value of α, we follow previous works focusing on the specific cases $\alpha = 0$ [40] and $\alpha = 1$ [42]. First, the reaction is assumed to take place only at the reaction front [40,42]. For large times compared to the characteristic reaction time, i.e., $t \gg 1$, the reaction is, indeed, limited by the diffusion of both reactants towards each other. The position z_f of the reaction front is moving on a diffusive timescale, i.e., $z_f = 2\,\eta_f\,\sqrt{t}$, where $\eta_f > 0$ is a constant [57,58]. Hence, A and B are consumed at the reaction front, and the concentration field of species I is a solution of the diffusive equation $\delta_I\, \frac{d^2 I}{d\eta^2} + 2\,\eta\, \frac{dI}{d\eta} = 0$, where $\delta_A = 1$, with the boundary condition

$$A = 1 - \alpha\,\gamma \quad \text{for } \eta = 0 \tag{9}$$

above the reaction front ($0 \leqslant \eta < \eta_f$), where $B = 0$ and $C = \gamma$, and boundary conditions

$$B \to \beta, \quad C \to 0 \quad \text{for } \eta \to \infty \tag{10}$$

below the reaction front ($\eta \geqslant \eta_f$), where $A = 0$. The asymptotic concentration fields are hence divided into two regions [40]. Above the reaction front, the asymptotic solutions denoted U (upper) are

$$A_U = (1 - \alpha\,\gamma)\left[1 - \frac{\mathrm{erf}(\eta)}{\mathrm{erf}(\eta_f)}\right], \tag{11a}$$

$$B_U = 0, \tag{11b}$$

$$C_U = \gamma, \tag{11c}$$

while those below the reaction front, denoted L (lower), read

$$A_L = 0, \tag{12a}$$

$$B_L = \beta\left[1 - \frac{\mathrm{erfc}\left(\frac{\eta}{\sqrt{\delta_B}}\right)}{\mathrm{erfc}\left(\frac{\eta_f}{\sqrt{\delta_B}}\right)}\right], \tag{12b}$$

$$C_L = \gamma\left[\frac{\mathrm{erfc}\left(\frac{\eta}{\sqrt{\delta_C}}\right)}{\mathrm{erfc}\left(\frac{\eta_f}{\sqrt{\delta_C}}\right)}\right], \tag{12c}$$

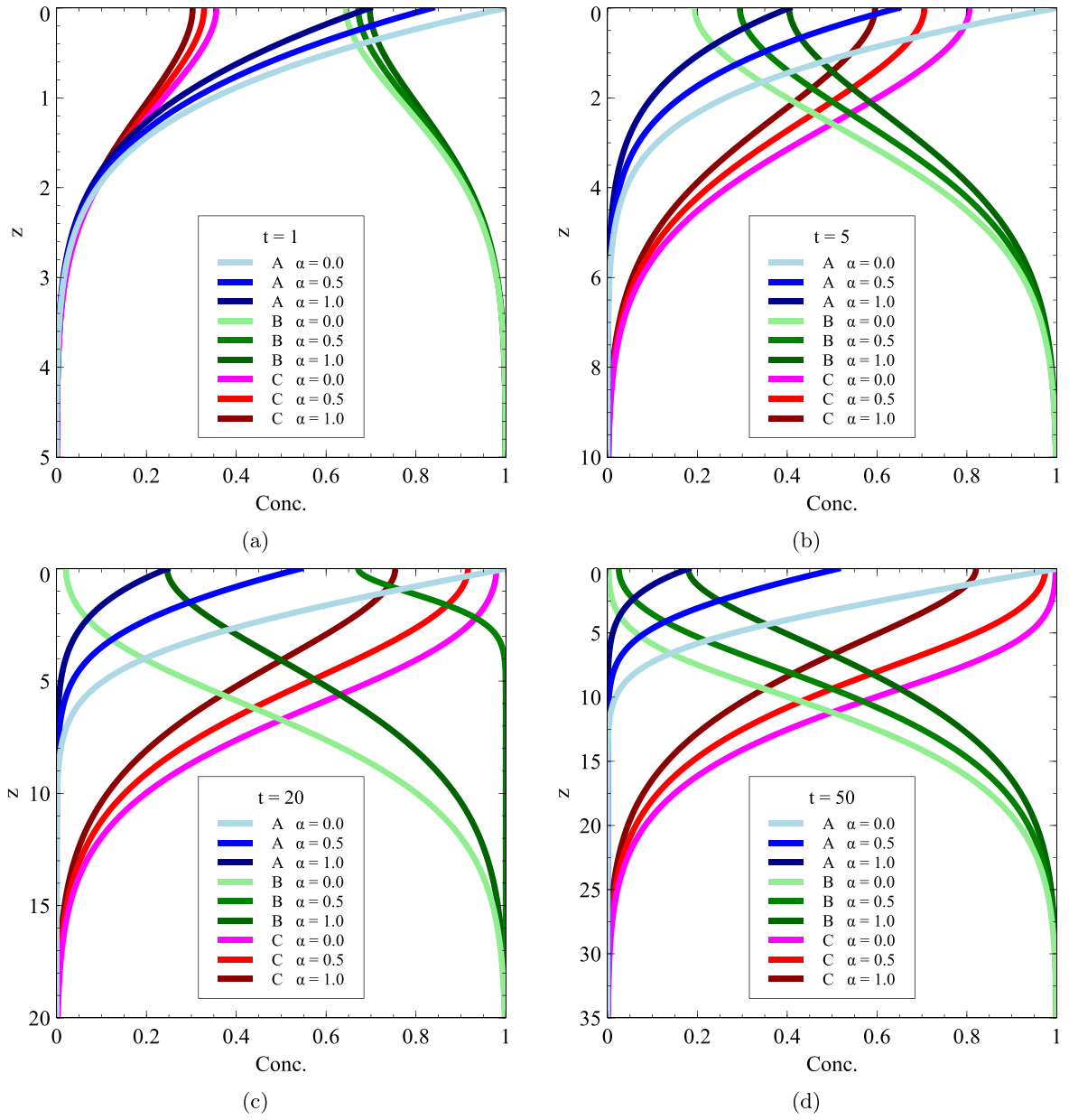

FIG. 2. RD concentration profiles for different values of α and $\beta = \delta_B = \delta_C = 1$ shown at four successive times: (a) $t = 1$, (b) $t = 5$, (c) $t = 20$, and (d) $t = 50$.

where $\mathrm{erfc}(\frac{\eta}{\sqrt{\delta_I}}) = 1 - \mathrm{erf}(\frac{\eta}{\sqrt{\delta_I}})$ is the complementary error function. In order to obtain the values of γ and η_f, we use the hypothesis that the reaction is limited by the diffusion of the species. Thus, the fluxes are equal at the reaction front, so that $\frac{dA_U}{d\eta}|_{\eta_f} = -\delta_B \frac{dB_L}{d\eta}|_{\eta_f} = \delta_C \frac{dC_L}{d\eta}|_{\eta_f}$. The value of C above the front γ and the position of the front η_f are solutions of a system of two equations [40,42]:

$$\gamma = \beta \frac{\sqrt{\delta_B}}{\sqrt{\delta_C}} \frac{\mathrm{erfc}\left(\frac{\eta_f}{\sqrt{\delta_C}}\right)}{\mathrm{erfc}\left(\frac{\eta_f}{\sqrt{\delta_B}}\right)} \exp\left[\eta_f^2 \left(\frac{1}{\delta_C} - \frac{1}{\delta_B}\right)\right], \quad (13a)$$

$$1 - \alpha\,\gamma = \beta \sqrt{\delta_B} \frac{\mathrm{erf}(\eta_f)}{\mathrm{erfc}\left(\frac{\eta_f}{\sqrt{\delta_B}}\right)} \exp\left[\eta_f^2 \left(1 - \frac{1}{\delta_B}\right)\right]. \quad (13b)$$

We compute γ and η_f as a function of those four parameters. Note that the position η_f of the reaction front therefore depends on α, β, δ_B, and δ_C, in contrast to previous work with $\alpha = 0$, where η_f was a function of only δ_B and β [40]. Therefore, Eqs. (11)–(13) provide the general form of the asymptotic concentration fields, where varying α allows the study of variable solubility, unifying different previous boundary conditions.

We first recall how γ and η_f depend on the parameters β, δ_B, and δ_C when $\alpha = 0$, as studied previously [40,44]. As A invades the host phase downwards from the interface where it dissolves, the reaction front always moves towards positive z and $\eta_f > 0$. The speed of the reaction front decreases (η_f decreases), and more C is produced (γ increases) if β or δ_B increases. Indeed, if reagent B is more concentrated or

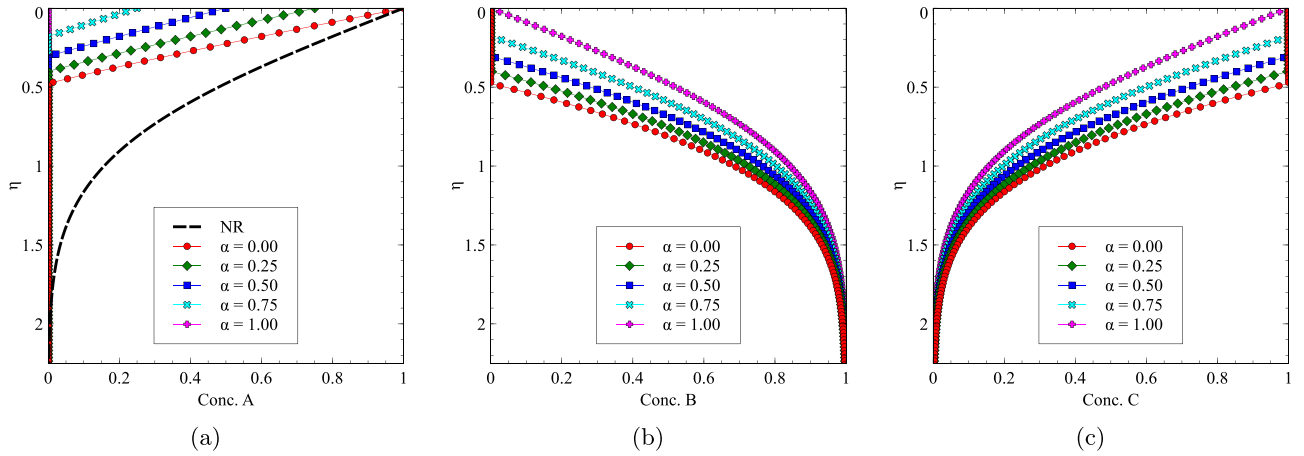

FIG. 3. Analytical asymptotic concentration profiles in the host phase for different values of α and $\beta = \delta_B = \delta_C = 1$: (a) reactant A (NR stands for nonreactive), (b) reactant B, and (c) product C.

diffuses more quickly towards the reactive zone, it increases the consumption of A and decreases the speed of its invasion of the host phase. Moreover, γ decreases if species C diffuses faster because it then accumulates less at the reaction front. Furthermore, $\gamma = \beta$ if all species diffuse at the same speed ($\delta_B = \delta_C$) [6,40,44]. Finally, it is important to note that the reaction front remains at the interface for small values of time. In these cases, only concentration profiles below the interface are considered [4].

The effect of varying α on the analytical asymptotic concentration profiles is presented in Fig. 3 for $\beta = \delta_B = \delta_C = 1$. First, note that the concentration of A is always smaller in the reactive cases than in the diffusive NR one. As we have assumed that A is directly and entirely consumed at the reaction front, its concentration varies from $1 - \alpha\, C$ at the interface to zero below the reaction front. The concentration of B is zero above the reaction front and increases in a monotonic way below the front up to the initial concentration β. Finally, product C accumulates in the system at a concentration γ above the reaction front and decreases diffusively below it. The larger α is, the more active the product C is in decreasing the solubility of A. There is, therefore, less A in the system when α increases. As a corollary, less B is consumed while less C is produced, and the position of the reaction front where the concentration of both reactants reaches zero is closer to the interface. In the case where $\alpha = 1$, the concentration of A is zero in the whole system because it is consumed as soon as it enters the system, with reactant B being present in excess. The concentration of C reaches its maximum value γ only at the interface, and its profile is then the same as the profile of A in the nonreactive case. We note that this ensues from the boundary condition $A + C = 1$ at the interface when $\alpha = 1$, implying that the solubility in the host phase fixes the total amount of A and C, independent of their chemical nature. The reaction, therefore, has no effect for $\alpha = 1$ on the system properties, as will be shown in the following sections.

2. *Position of the reaction front*

The position of the reaction front is defined as the position z_f where the reaction rate $R = A\,B$ is maximum. This position coincides with the point where $A = B$ when $\delta_B = \delta_C = 1$. Over time, the reaction front moves in the direction $z > 0$, and its position z_f evolves according to a diffusive timescale $\sqrt{t}$. As shown in Fig. 4(a), if α increases, the reaction front advances less rapidly in the system. For $\alpha = 1$, the front remains stuck at the interface ($z_f = 0$).

We observe that, for intermediate values of α, the reaction front remains at the interface for a certain time before first moving further in the system and then moving diffusively. This jump can be explained by the definition of the position of the reaction front. As illustrated in Fig. 4(b) for the case $\alpha = 0.5$, we observe that, at shorter times (here $t = 10$), R is maximum at the interface, and $z_f = 0$. It is only after a longer dimensionless time, $t = 45$, for instance, that the reaction rate at the interface becomes smaller than the maximum value in the bulk. At this moment, the position z_f starts to move. As the reaction takes place for a longer time close to the interface when α increases, this explains the longer delay of the jump away from the interface when α increases. As stated above, if $\alpha = 1$, the reaction front remains at the interface at all times [42,43].

3. *Flux of A through the interface*

In the context of partially miscible systems such as CO_2 sequestration or in general for any dissolution of a phase in another one, the flux of A through the interface defined as $J = -\frac{\partial A}{\partial z}|_{z=0}$ is an important quantity to compute. We recall that, for the nonreactive case, the analytical flux $J_{\rm NR} = \frac{1}{\sqrt{\pi\, t}}$. In the asymptotic limit, the flux in the reactive case is

$$J = -\left.\frac{\partial A_U}{\partial z}\right|_{z=0} = \frac{1-\alpha\,\gamma}{\mathrm{erf}(\eta_f)\,\sqrt{\pi\, t}} = \frac{(1-\alpha\,\gamma)\,J_{\rm NR}}{\mathrm{erf}(\eta_f)}. \quad (14)$$

Figure 5 shows the temporal evolution of the flux for different values of α in the reactive case. When $\alpha = 0$, the flux is increased by the reaction, as shown previously [46,48]. However, when α increases, C hinders the dissolution of A, and the flux decreases, tending to the value of the nonreactive case for $\alpha = 1$. This is logical because, for $\alpha = 1$, A is fully

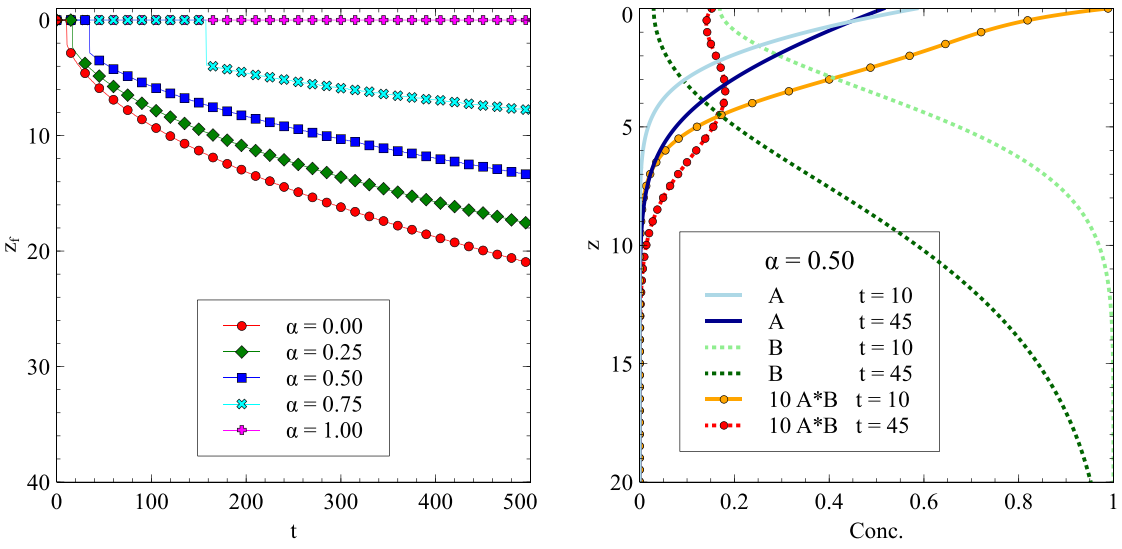

FIG. 4. (a) Temporal evolution of the position z_f of the reaction front for $\beta = \delta_B = \delta_C = 1$ and different values of α; (b) concentration profiles for $\alpha = 0.50$ at dimensionless times of 10 and 45.

converted into C and the asymptotic profile of C equals the nonreactive profile of A.

4. Total amount of dissolved A

In order to estimate the storage capacity of a host phase, we compute the dissolved amount of each species in the solution as a function of time. For the nonreactive case, the total amount of A dissolved in the host solution $||A_{\mathrm{NR}}||$ can be calculated analytically, according to Eq. (15), by integrating the concentration profile in space,

$$||A_{\mathrm{NR}}|| = \int_0^{L_z} \left[1 - \mathrm{erf}\left(\frac{z}{2\sqrt{t}}\right)\right] dz = -L_z\,\mathrm{erf}\left(\frac{L_z}{2\sqrt{t}}\right) - \frac{2\sqrt{t}\left[\exp\left(-\frac{L_z^2}{4t}\right) - 1\right]}{\sqrt{\pi}} + L_z, \tag{15}$$

where L_z is the length of the system. In the reactive cases, the dissolved quantity of each species $||I||$ is computed numerically as

$$||I|| = \int_0^{L_z} I(z)\,dz. \tag{16}$$

With A being transformed into C by reaction, the total amount of A dissolved in the host phase is the sum of the amount of A and that of C, the temporal evolution of which is represented in Fig. 6 for five values of α. When α increases, the total amount of A dissolved in the host phase decreases as the flux of A decreases. When $\alpha = 1$, we recover again the values of the NR case, i.e., $||A|| + ||C|| = ||A_{\mathrm{NR}}||$.

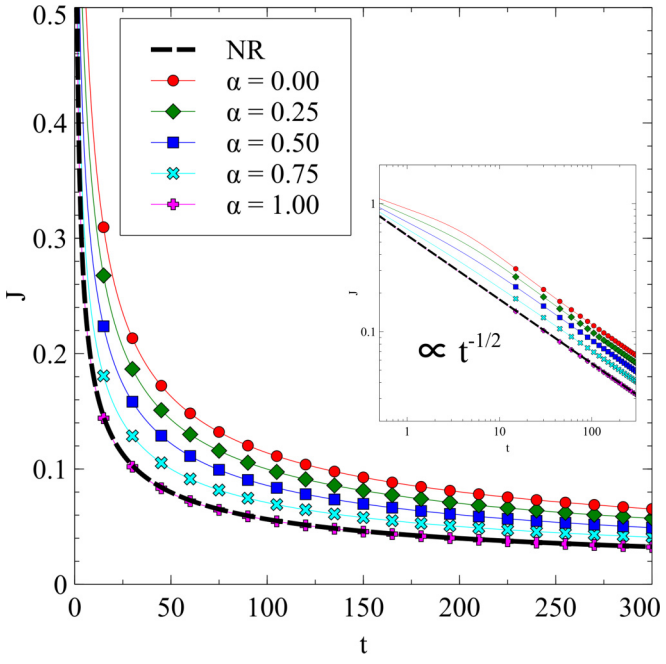

FIG. 5. Temporal evolution of the flux of A through the interface ($z = 0$) for different values of α and $\beta = \delta_B = \delta_C = 1$ compared to the nonreactive (NR) case. The inset presents the same evolution on a log-log scale.

C. Parametric study

We now study numerically for variable α the influence of varying the other parameters of the system (β, δ_B, and δ_C) on the interfacial concentration of A and on its flux through the interface given by Eq. (14). The results are illustrated in Fig. 7, where the scales used are different depending on the studied parameter for the sake of visual clarity.

For a given value of α, the solubility of A decreases when β increases since more C is produced. Conversely, $A(z = 0)$ decreases when α increases for a given value of β. We note that the flux of A is not affected by α for small values of β. This important result shows that if the host phase is not very

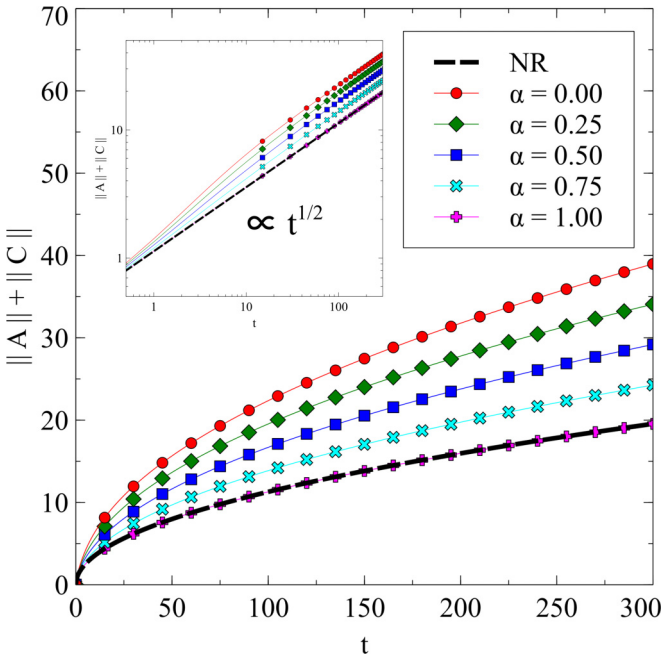

FIG. 6. Temporal evolution of the total amount of A dissolved in the host phase either as reactant A or product C for different values of α and $\beta = \delta_B = \delta_C = 1$ compared to the nonreactive (NR) case. The inset features the same evolution on a log-log scale.

concentrated in B the flux of A is not limited by the reaction, but mainly by its diffusion. Therefore, to improve the transfer of A to the host phase, it is best to use a concentrated host phase, even if its solubility is reduced by the reaction product.

For small values of α, varying δ_B, the diffusivity of B, does not affect the solubility of A much. Since the production of C is enhanced with an increase of δ_B, the solubility of A is decreased when δ_B increases for high values of α. However, it is consumed faster at the interface, and its flux is increased. Even if this result is less marked for high values of α, it explains the fact that an increase in the diffusivity of B improves the transfer by consuming A and allowing more of it to enter the system. This effect is observable for any value of $\alpha < 1$.

When $\alpha = 0$, the diffusion of the product has no effect on either the solubility of A or its flux. However, if $\alpha \neq 0$, for high values of δ_C, the solubility of A and its flux are enhanced because C is then less present near the interface. Conversely, for small values of δ_C, the product stays near the interface and hinders the dissolution of A. Hence, its solubility and its flux are the smallest for small values of δ_C and high values of α with possibility of having $J < J_{\mathrm{NR}}$ in some cases [see Fig. 7(f)].

To summarize, the mass transfer to the host phase is improved with a higher initial concentration of reactant B and a higher diffusivity of species B and C compared to that of A.

IV. DISCUSSION

A. Dynamics at the interface

The production of C at the interface is limited by the concentration of B at the interface when its initial concentration is lower than that of A. Thus, when all species diffuse at the same rate, $A(z = 0)$ and $C(z = 0)$ tend to $1 - \alpha\,\beta$ and β, respectively, if $\beta < 1$. On the other hand, when A is the minority species, the production of C is limited by the presence of A and therefore by its flux. The concentration of C at the interface rapidly exceeds that of A, tending towards β. If the reactant B diffuses faster than A ($\delta_B > 1$), the formation of the product is again limited by the presence of A. If C diffuses more slowly than A, it accumulates close to the interface, and its concentration increases there, exceeding β. For high values of α and small values of δ_C, the concentration of C has such an impact on the solubility of A that its flow through the interface even becomes smaller than in the absence of reaction, reducing the efficiency of the mass transfer: $J < J_{\mathrm{NR}}$ [see Fig. 7(f)].

To summarize, when $\alpha = 0$, the solubility of A is constant, and the flux $J > J_{\mathrm{NR}}$, while when increasing $\alpha > 0$, the solubility and the flux of A decrease, tending to the nonreactive value when $\alpha = 1$. Previous works showed that the flux is a function of δ_B and β when $\alpha = 0$ [40,48] and a function of δ_C when $\alpha = 1$ [42,43]. In this work, we unified the boundary conditions regarding the solubility of A and showed how J is a function of β, δ_B, δ_C, and α.

B. Dynamics in the solution

The reaction A + B → C occurs in the reaction front, which is located at the interface at short times and invades the host phase later on.

As α increases, the flux of A decreases, the reaction front is closer to the interface, and the dissolved amount of A present in the solution decreases and tends to zero. The amount of C in solution also decreases when α increases and is bounded by the total amount of A in the absence of reaction for $\alpha = 1$. In the latter case, the reaction front stays at the interface.

C. Application to CO_2 sequestration

In order to increase the safety of the CO_2 sequestration process, it is preferable for the reaction to take place as quickly as possible at depths farther from the interface (solubility trapping). Moreover, it is desirable to have higher values of the CO_2 flux through the interface and optimize the total quantity of CO_2 that can be dissolved. We showed that the influence on CO_2 solubility of the product of the reaction between CO_2 and possible reactants needs to be considered. In the case of CO_2 dissolution in saline aquifers, reactions have been shown to affect dissolution-driven convection. The general boundary condition used here for CO_2 solubility could modify the classification of the effect of chemical reactions on CO_2 convective dissolution.

V. CONCLUSIONS

We have computed theoretically the reaction-diffusion concentration profiles of species A, B, and C in a partially miscible system in which a reaction A + B → C occurs in the host phase when the solubility of A linearly decreases with the concentration of the reaction product as $A(z = 0) = 1 - \alpha\,C$. The mass transfer of A to the host phase is enhanced by the chemical reaction consuming A for $0 \leqslant \alpha < 1$. If the influence of C on the variable solubility of A increases, i.e., α

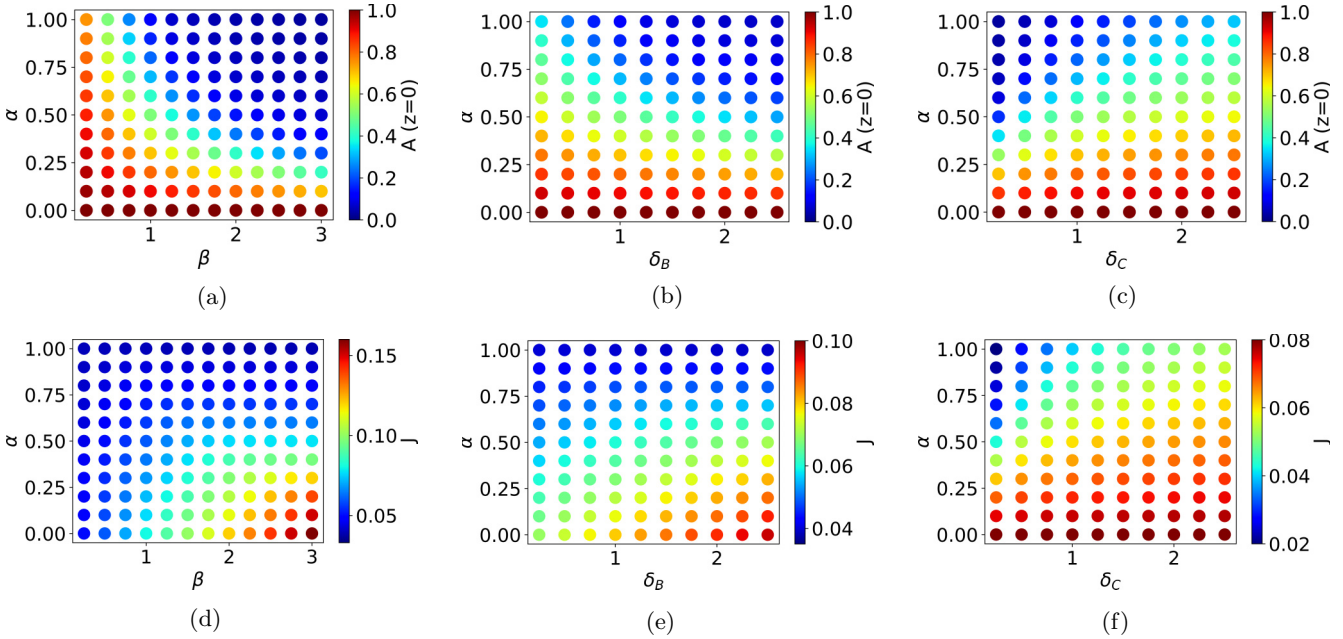

FIG. 7. Influence of the parameters β, δ_B, and δ_C as a function of α on the solubility of A and on the flux J of A through the interface at a dimensionless time of 300 [$J_{\mathrm{NR}}(t = 300) = 0.03257$]. In these parameter spaces, the key parameter α varies in the range $0 \leqslant \alpha \leqslant 1$ on the vertical axis. On the horizontal axis, the second parameter, β, δ_B, or δ_C, varies between 0 and 3 while the other parameters are set to 1. The values of the solubility and the flux are presented as a colored scatterplot between low values in blue and high values in red. Therefore, the red areas correspond to parameter values that optimize the solubility of A and increase the flux. Specifically, the panels show the influence of α and of (a) β on $A(z = 0)$ ($\delta_B = \delta_C = 1$), (b) δ_B on $A(z = 0)$ ($\beta = \delta_C = 1$), (c) δ_C on $A(z = 0)$ ($\beta = \delta_B = 1$), (d) β on J ($\delta_B = \delta_C = 1$), (e) δ_B on J ($\beta = \delta_C = 1$), and (f) δ_C on J ($\beta = \delta_B = 1$).

increases, the reaction front advances more slowly in the host phase. In the limit $\alpha = 1$, A is consumed as soon as it enters the system, the reaction front remains at the interface, and we recover the nonreactive case as the spatial dependence of C is the same as the diffusive profile of A in the nonreactive case. With regard to the flux, the largest value is obtained for $\alpha = 0$. If α increases, the flux of A through the interface decreases and tends to the flux in the nonreactive case, meaning that the chemical reaction no longer improves the mass transfer. Finally, we have analyzed the impact on the reactive system of varying the ratio β of the initial reactant concentration and solubility of A and the diffusivity ratios δ_B and δ_C for variable α. For a fixed value of α, the mass transfer from the reservoir phase A to the host phase is enhanced by increasing β, δ_B, and δ_C. This increase of the mass transfer is limited by the influence of C on the solubility of A: when α increases, the mass transfer decreases. Nevertheless, the first effect dominates over the second one, as we have shown it is best to use a concentrated reactive host phase to improve the mass transfer of A and the total amount being dissolved even if the reaction product decreases the solubility of A. When $\alpha \to 1$, the flux J can become smaller than J_{NR} for larger values of δ_C.

This study opens perspectives for future research. In addition to the influence of C on $A(z = 0)$, the spatiotemporal evolution of the concentration of B could also have an impact on the local solubility of A. Related RD profiles could be studied along the lines of the current study. Moreover, with the density profile at the source of buoyancy-driven convection being directly correlated to the concentration fields, this study provides the RD concentration profiles that can serve as a basis for a better understanding of density base state profiles needed to investigate the effect of variable solubility on CO_2 convective dissolution.

ACKNOWLEDGMENT

We acknowledge the financial support of ULB as well as of the ARC program via the project CREDI and the Fondation ULB.

[1] A. C. Slim, M. M. Bandi, J. C. Miller, and L. Mahadevan, Dissolution-driven convection in a Hele-Shaw cell, Phys. Fluids **25**, 024101 (2013).

[2] J. Philippi, M. Berhanu, J. Derr, and S. Courrech du Pont, Solutal convection induced by dissolution, Phys. Rev. Fluids **4**, 103801 (2019).

[3] M. A. Bees, A. J. Pons, P. G. Sørensen, and F. Sagués, Chemoconvection: A chemically driven hydrodynamic instability, Chem. Phys. **114**, 1932 (2001).

[4] C. Wylock, A. Rednikov, B. Haut, and P. Colinet, Nonmonotonic Rayleigh-Taylor instabilities driven by gas-liquid CO_2 chemisorption, J. Phys. Chem. B **118**, 11323 (2014).

[5] C. Wylock, A. Rednikov, P. Colinet, and B. Haut, Experimental and numerical analysis of buoyancy-induced instability during CO_2 absorption in $NaHCO_3$-Na_2CO_3 aqueous solutions, Chem. Eng. Sci. **157**, 232 (2017).

[6] V. Loodts, C. Thomas, L. Rongy, and A. De Wit, Control of Convective Dissolution by Chemical Reactions: General Classification and Application to CO_2 Dissolution in Reactive Aqueous Solutions, Phys. Rev. Lett. **113**, 114501 (2014).

[7] A. Vreme, F. Nadal, B. Pouligny, P. Jeandet, G. Liger-Belair, and P. Meunier, Gravitational instability due to the dissolution of carbon dioxide in a Hele-Shaw cell, Phys. Rev. Fluids **1**, 064301 (2016).

[8] C. Thomas, S. Dehaeck, and A. De Wit, Convective dissolution of CO_2 in water and salt solutions, Int. J. Greenhouse Gas Control **72**, 105 (2018).

[9] H. Liu and A. F. Taylor, Influence of oxygen on chemoconvective patterns in the iodine clock reaction, J. Phys. Chem. B **126**, 10136 (2022).

[10] M. A. Budroni, C. Thomas, and A. De Wit, Chemical control of dissolution-driven convection in partially miscible systems: Nonlinear simulations and experiments, Phys. Chem. Chem. Phys. **19**, 7936 (2017).

[11] M. A. Budroni, L. A. Riolfo, L. Lemaigre, F. Rossi, M. Rustici, and A. De Wit, Chemical control of hydrodynamic instabilities in partially miscible two-layer systems, J. Phys. Chem. Lett. **5**, 875 (2014).

[12] K. Eckert and A. Grahn, Plume and Finger Regimes Driven by an Exothermic Interfacial Reaction, Phys. Rev. Lett. **82**, 4436 (1999).

[13] R. Sczech, K. Eckert, and M. Acker, Convective instability in a liquid-liquid system due to complexation with a crown ether, J. Phys. Chem. A **112**, 7357 (2008).

[14] S. S. S. Cardoso and J. T. H. Andres, Geochemistry of silicate-rich rocks can curtail spreading of carbon dioxide in subsurface aquifers, Nat. Commun. **5**, 5743 (2014).

[15] I. Cherezov and S. S. S. Cardoso, Acceleration of convective dissolution by chemical reaction in a Hele-Shaw cell, Phys. Chem. Chem. Phys. **18**, 23727 (2016).

[16] A. Riaz, M. Hesse, H. A. Tchelepi, and F. M. Orr, Onset of convection in a gravitationally unstable diffusive boundary layer in porous media, J. Fluid Mech. **548**, 87 (2006).

[17] D. P. Schrag, Preparing to capture carbon, Science **315**, 812 (2007).

[18] S. Bachu, CO_2 storage in geological media: Role, means, status and barriers to deployment, Prog. Energy Combust. Sci. **34**, 254 (2008).

[19] J. A. Neufeld and H. E. Huppert, Modelling carbon dioxide sequestration in layered strata, J. Fluid Mech. **625**, 353 (2009).

[20] M. T. Elenius and K. Johannsen, On the time scales of nonlinear instability in miscible displacement porous media flow, Comput. Geosci. **16**, 901 (2012).

[21] A. C. Slim, Solutal-convection regimes in a two-dimensional porous medium, J. Fluid Mech. **741**, 461 (2014).

[22] H. E. Huppert and J. A. Neufeld, The fluid mechanics of carbon dioxide sequestration, Annu. Rev. Fluid Mech. **46**, 255 (2014).

[23] H. Emami-Meybodi, H. Hassanzadeh, C. P. Green, and J. Ennis-King, Convective dissolution of CO_2 in saline aquifers: Progress in modeling and experiments, Int. J. Greenhouse Gas Control **40**, 238 (2015).

[24] L. Rongy, K. B. Haugen, and A. Firoozabadi, Mixing from Fickian diffusion and natural convection in binary non-equilibrium fluid phases, AIChE J. **58**, 1336 (2012).

[25] T. J. Kneafsey and K. Pruess, Laboratory flow experiments for visualizing carbon dioxide-induced, density-driven brine convection, Transp. Porous Media **82**, 123 (2010).

[26] T. F. Faisal, S. Chevalier, and M. Sassi, Experimental and numerical studies of density driven natural convection in saturated porous media with application to CO_2 geological storage, Energy Procedia **37**, 5323 (2013).

[27] R. Outeda, C. El Hasi, A. D'Onofrio, and A. Zalts, Experimental study of linear and nonlinear regimes of density-driven instabilities induced by CO_2 dissolution in water, Chaos **24**, 013135 (2014).

[28] C. Thomas, L. Lemaigre, A. Zalts, A. D'Onofrio, and A. De Wit, Experimental study of CO_2 convective dissolution: The effect of color indicators, Int. J. Greenhouse Gas Control **42**, 525 (2015).

[29] C. Thomas, V. Loodts, L. Rongy, and A. De Wit, Convective dissolution of CO_2 in reactive alkaline solutions: Active role of spectator ions, Int. J. Greenhouse Gas Control **53**, 230 (2016).

[30] J. Ennis-King and L. Paterson, Coupling of geochemical reactions and convective mixing in the long-term geological storage of carbon dioxide, Int. J. Greenhouse Gas Control **1**, 86 (2007).

[31] J. T. H. Andres and S. S. S. Cardoso, Onset of convection in a porous medium in the presence of chemical reaction, Phys. Rev. E **83**, 046312 (2011).

[32] K. Ghesmat, H. Hassanzadeh, and J. Abedi, The impact of geochemistry on convective mixing in a gravitationally unstable diffusive boundary layer in porous media: CO_2 storage in saline aquifers, J. Fluid Mech. **673**, 480 (2011).

[33] Y. Jun, D. E. Giammar, and C. J. Werth, Impacts of geochemical reactions on geologic carbon sequestration, Environ. Sci. Technol. **47**, 3 (2013).

[34] L. Binda, C. El Hasi, A. Zalts, and A. D'Onofrio, Experimental analysis of density fingering instability modified by precipitation, Chaos **27**, 053111 (2017).

[35] C. Thomas, S. Dehaeck, and A. De Wit, Effect of precipitation mineralization reactions on convective dissolution of CO_2: An experimental study, Phys. Rev. Fluids **5**, 113505 (2020).

[36] V. Loodts, L. Rongy, and A. De Wit, Impact of pressure, salt concentration, and temperature on the convective dissolution of carbon dioxide in aqueous solutions, Chaos **24**, 043120 (2014).

[37] S. M. Jafari Raad, H. Emami-Meybodi, and H. Hassanzadeh, Impact of boundary excitation on stability of a diffusive boundary layer in porous media, Adv. Water Resour. **126**, 40 (2019).

[38] J. Wang, Z. Wang, D. Ryan, and C. Lan, A study of the effect of impurities on CO_2 storage capacity in geological formations, Int. J. Greenhouse Gas Control **42**, 132 (2015).

[39] S. M. Jafari Raad and H. Hassanzadeh, Prospect for storage of impure carbon dioxide streams in deep saline aquifers—A convective dissolution perspective, Int. J. Greenhouse Gas Control **63**, 350 (2017).

[40] V. Loodts, P. M. J. Trevelyan, L. Rongy, and A. De Wit, Density profiles around $A + B \rightarrow C$ reaction-diffusion fronts in partially miscible systems: A general classification, Phys. Rev. E **94**, 043115 (2016).

[41] P. Ghoshal and S. S. S. Cardoso, Reactive convective-dissolution in a porous medium: Stability and nonlinear dynamics, Phys. Chem. Chem. Phys. **20**, 21617 (2018).

[42] M. C. Kim and S. S. S. Cardoso, Diffusivity ratio effect on the onset of the buoyancy-driven instability of an A + B → C chemical reaction system in a Hele-Shaw cell: Asymptotic and linear stability analyses, Phys. Fluids **30**, 094102 (2018).

[43] M. C. Kim and S. S. S. Cardoso, Diffusivity ratio effect on the onset of the buoyancy-driven instability of an A + B → C chemical reaction system in a Hele-Shaw cell: Numerical simulations and comparison with experiments, Phys. Fluids **31**, 084101 (2019).

[44] V. Loodts, L. Rongy, and A. De Wit, Chemical control of dissolution-driven convection in partially miscible systems: Theoretical classification, Phys. Chem. Chem. Phys. **17**, 29814 (2015).

[45] V. Loodts, H. Saghou, B. Knaepen, L. Rongy, and A. De Wit, Differential diffusivity effects in reactive convective dissolution, Fluids **3**, 83 (2018).

[46] M. Jotkar, A. De Wit, and L. Rongy, Enhanced convective dissolution due to an A + B → C reaction: Control of the nonlinear dynamics via solutal density contributions, Phys. Chem. Chem. Phys. **21**, 6432 (2019).

[47] M. Jotkar, L. Rongy, and A. De Wit, Reactive convective dissolution with differential diffusivities: Nonlinear simulations of onset times and asymptotic fluxes, Phys. Rev. Fluids **5**, 104502 (2020).

[48] V. Loodts, B. Knaepen, L. Rongy, and A. De Wit, Enhanced steady-state dissolution flux in reactive convective dissolution, Phys. Chem. Chem. Phys. **19**, 18565 (2017).

[49] P. Ghoshal, M. C. Kim, and S. S. S. Cardoso, Reactive-convective dissolution in a porous medium: The storage of carbon dioxide in saline aquifers, Phys. Chem. Chem. Phys. **19**, 644 (2017).

[50] W. Yan, S. Huang, and E. H. Stenby, Measurement and modeling of CO_2 solubility in NaCl brine and CO_2-saturated NaCl brine density, Int. J. Greenhouse Gas Control **5**, 1460 (2011).

[51] W. M. Haynes, D. R. Lide, and T. J. Bruno, *CRC Handbook of Chemistry and Physics 2012-2013* (CRC Press, London, 2012).

[52] V. Savary, G. Berger, M. Dubois, J.-C. Lacharpagne, A. Pages, S. Thibeau, and M. Lescanne, The solubility of $CO_2 + H_2S$ mixtures in water and 2 M NaCl at 120 °C and pressures up to 35 MPa, Int. J. Greenhouse Gas Control **10**, 123 (2012).

[53] H. Zhao, R. M. Dilmore, and S. N. Lvov, Experimental studies and modeling of CO_2 solubility in high temperature aqueous $CaCl_2$, $MgCl_2$, Na_2SO_4, and KCl solutions, AIChE J. **61**, 2286 (2015).

[54] R. Khosrokhavar, G. Elsinga, R. Farajzadeh, and H. Bruining, Visualization and investigation of natural convection flow of CO_2 in aqueous and oleic systems, J. Pet. Sci. Eng. **122**, 230 (2014).

[55] L. Rongy, P. M. J. Trevelyan, and A. De Wit, Dynamics of $A + B \rightarrow C$ Reaction Fronts in the Presence of Buoyancy-Driven Convection, Phys. Rev. Lett. **101**, 084503 (2008).

[56] L. Rongy, P. M. J. Trevelyan, and A. De Wit, Influence of buoyancy-driven convection on the dynamics of A + B → C reaction fronts in horizontal solution layers, Chem. Eng. Sci. **65**, 2382 (2010).

[57] L. Gálfi and Z. Rácz, Properties of the reaction front in an $A + B \rightarrow C$ type reaction-diffusion process, Phys. Rev. A **38**, 3151 (1988).

[58] Z. Jiang and C. Ebner, Simulation study of reaction fronts, Phys. Rev. A **42**, 7483 (1990).